June 19, 1969

TM-180
0424

Magnetic Measurements on the Model Main Ring Quadrupole

J.F. Schivell

Introduction

We present the results of studying the magnetic field quality in the two-dimensional region of the model main ring quadrupole. We describe how the measurements were made, and compare the results with the designed quality of the field. A comparison is made between certain field errors and the mechanical inperfections which appear to have caused them. Also, the accuracy of the design-aiding program LINDA is verified for this case down to a certain level.

Construction of the Model

The designs for the laminations and the coils for this model were finished before July, 1968. The lamination is equivalent to case 263606 run with LINDA (drawing No. 200E194B) and the coil is that specified in drawings No. 200E683-685.

Each half core of the model is a 3 foot stack of laminations, held in compression by long bolts through the end plates. The two half cores are held together by four bolts, one at each corner of the magnet.

The first set of coils to arrive was installed in the quadrupole only after considerable difficulty, including sanding off excess insulation and finally forcing the coils into the half cores. When the halves of the magnet had been bolted together there was a gap between the half cores of as much as .010 inch. When the second set of coils arrived, these were installed in the magnet with much less difficulty, but there remained a gap of several thousandths of an inch apparently due to the coils being oversize. The measurements reported below were all made with the second set of coils. The dimensional errors in the magnet are discussed more quantitatively below.

Method of Describing the Magnetic Field

The magnetic field will be described by giving its multipole components. If a magnetic scaler potential which satisfies Laplace's equation is expanded in a cylindrical coordinate system, then

$$V_m = \sum_{n=0}^{\infty} r^n \left(\phi_{n,1} \cos n\,\theta + \phi_{n,2} \sin n\,\theta\right),$$

where the $\phi_{n,i}$ (i=1,2) are the multipole coefficients. The tolerances on the field quality can be expressed as limits on the $\phi_{n,i}$. Also, the output of LINDA can readily be converted to these terms, and the $\phi_{n,i}$ can be measured directly by the apparatus we have used.

Field Measuring Equipment

The principle device used for measuring the field is shown in Fig. 1. There were two search coils wound on rectangular Pyrex forms, each form 4 inch x 0.4 inch x 0.5 inch. Each was wound with 190 turns of .002 inch wire. Both coils were held in a box, on the same side of the axis of rotation. Both coils were oriented so as to measure field in the radial direction. On each large face of the box, on either side of coil C_1, was a 2-turn trimming coil which was sensitive to B_θ. All four coils were summed through resistors and connected to an integrator by the circuit shown in Fig. 2. The output of the integrator was fed to an A-to-D channel of the magnet measurements Varian 620/i computer. The search coil box was supported on a 6 foot long ceramic boom. The box was rotated by a ceramic shaft inside the boom, turned at the other end by a 200 step/circle stepping motor. Data were normally taken at 40 different positions around a circle - that is, every 9 degrees.

The measurements reported here were taken while the magnet was being pulsed on a cycle similar to that of the main ring. However, to the accuracy of these measurements, the result is the same as though the magnet had been on DC excitation. The choice of using pulsed conditions was for practice and convenience in measuring at several values of the current on the same run. Due to problems with noise in the current shunt, we did not use it, but rather sensed the level of excitation by means of a small, fixed search coil in the quadrupole gap connected to an integrator. The integrator output was calibrated by reading the ammeter on the power supply, which gave sufficient accuracy for our present purposes.

The measuring cycle is diagrammed in Fig. 3.

The data were recorded on magnetic tape and Fourier analyzed later on the IBM 360 at Argonne. The results presented below are the combination of 8 runs (360° rotation each), all taken with the search coils located so as to measure the field at 9 ± 2 inches from the quadrupole end face which was opposite the end with the power and water connections. This particular search coil location was favored because it was far enough inside the magnet to be away from end effects, yet it was fairly easily accessible for mechanical measurements of the magnet deformations.

Results

The multipole coefficients measured at 1050 Amps are given in Table 1. The first two columns are $\phi_{n,1}$ and $\phi_{n,2}$, the cosine and sine coefficients, respectively. The third column gives the modulus of each multipole, that is $[\phi_{n,1}{}^2 + \phi_{n,2}{}^2]^{1/2}$. The uncertainties quoted are the r.m.s. deviations for the 8 runs. The fourth column contains the values of the multipoles calculated with LINDA. We have been careful to adjust all signs so that measured and LINDA values apply to the same origin and sense of angle and the same sign of exciting currents. The units are Gauss/cm^{n-1}.

Tolerances for the n=4, 6, and 8 coefficients in the quadrupole have been calculated by finding the betatron phase shift caused by each.[1] They are as follows:

n	Limit on $\phi_{n,2}$
4	1.48×10^{-2}
6	6.38×10^{-4}
8	4.37×10^{-5}

The multipole coefficients calculated by LINDA are within the tolerances by a factor of 2, but the measured values exceed the tolerances by a significant factor.

A probable explanation for most of the large error in the field lies in the mechanical flexing and "breathing" of the quadrupole. To investigate this effect a study was made of the actual locations of the poles with respect to one another and of the octupole moment as a function of current. (The octupole is most sensitive to motion of the poles.)

Using a bronze sliding parallel, the distance was measured between the two flat surfaces forming the narrowest part of the quadrupole gap on either side of the magnet. (Since there is little flat area not covered by the coils, the parallel was held as close as possible to the coil.) The gap was measured at roughly the same place in the magnet where the magnetic data were taken. The gap was measured with the magnet current off and at 5 values up to 1150 Amps. In Table 2 are the results, along with predicted values of $\phi_{4,2}/I$, obtained from these data and LINDA calculations.[2]

Figure 4 shows $\phi_{4,2}/I$, where I is the magnet current, as function of I, from the following:

1) the measured data from the model quadrupole,

2) the prediction of LINDA for the case with the poles in the right place,

3) the prediction of LINDA for moving poles (Table 2), and

4) the tolerance on the amount of octupole.[1]

The amount of agreement between 3) and 1) suggests that most of the error in the quadrupole field can be removed by removing the backleg gap and also by preventing the poles from flexing in at high fields.

Also, LINDA appears to work reasonably well in the case of this quadrupole, at least to the precision to which we have measured.

Footnotes

[1] F.C. Shoemaker, private communication

[2] See "Studies of the Main Ring Quadrupole with the LINDA Program", J.F. Schivell, to be published.

Table 1

Measured and Calculated Multipole Coefficients

n	$\phi_{n,1}$	$\phi_{n,2}$	$\lvert\phi_n\rvert$	LINDA ($\phi_{n,2}$)
3	$(-1.82 \pm 0.34) \times 10^{-1}$	$(-1.51 \pm 0.31) \times 10^{-1}$	$(2.39 \pm 0.26) \times 10^{-1}$	
4	$(-1.43 \pm 4.08) \times 10^{-3}$	$(-2.13 \pm 0.56) \times 10^{-2}$	$(2.18 \pm 0.57) \times 10^{-2}$	$+8.16 \times 10^{-3}$
5	$(0.08 \pm 9.99) \times 10^{-4}$	$(-2.08 \pm 0.83) \times 10^{-3}$	$(2.35 \pm 0.69) \times 10^{-3}$	
6	$(3.88 \pm 3.41) \times 10^{-4}$	$(-1.57 \pm 0.45) \times 10^{-3}$	$(1.67 \pm 0.41) \times 10^{-3}$	-4.3×10^{-4}
7	$(0.18 \pm 1.08) \times 10^{-4}$	$(-1.39 \pm 0.69) \times 10^{-4}$	$(1.75 \pm 0.73) \times 10^{-4}$	
8	$(2.70 \pm 2.11) \times 10^{-5}$	$(-6.08 \pm 2.82) \times 10^{-5}$	$(7.22 \pm 2.15) \times 10^{-5}$	-2.17×10^{-5}
9	$(-1.35 \pm 5.09) \times 10^{-6}$	$(0.48 \pm 1.56) \times 10^{-5}$	$(1.38 \pm 1.01) \times 10^{-5}$	
10	$(2.42 \pm 2.33) \times 10^{-6}$	$(-1.80 \pm 2.59) \times 10^{-6}$	$(3.91 \pm 2.45) \times 10^{-6}$	-2.29×10^{-6}
11	$(-1.99 \pm 5.74) \times 10^{-7}$	$(0.45 \pm 1.01) \times 10^{-6}$	$(1.09 \pm 0.64) \times 10^{-6}$	
12	$(1.50 \pm 3.82) \times 10^{-7}$	$(1.92 \pm 3.43) \times 10^{-7}$	$(4.69 \pm 3.21) \times 10^{-7}$	-9.93×10^{-8}
13	$(-2.83 \pm 7.36) \times 10^{-8}$	$(2.32 \pm 8.77) \times 10^{-8}$	$(1.08 \pm 0.54) \times 10^{-7}$	
14	$(0.60 \pm 3.90) \times 10^{-8}$	$(-0.11 \pm 2.72) \times 10^{-8}$	$(4.12 \pm 2.44) \times 10^{-8}$	-2.78×10^{-9}
15	$(-0.06 \pm 1.31) \times 10^{-8}$	$(-0.52 \pm 1.53) \times 10^{-8}$	$(1.97 \pm 0.67) \times 10^{-8}$	

Table 2

Side gap errors and predicted octupole

(gap nominal value 0.900 in.)

I (amp)	Δg (mils)	$\phi_{4,2}/I$ (G/cm^3 Amp)
0	+ 6.5	4.9×10^{-5}
179	+ 7.0	5.3×10^{-5}
448	+ 2.75	2.3×10^{-5}
716	0	0.4×10^{-5}
985	− 2	-0.5×10^{-5}
1150	− 2	-0.5×10^{-5}

Note - due to the difficulty of measuring Δg, there is an uncertainty in $\phi_{4,2}/I$ of $\pm\ 0.7 \times 10^{-5}$ G/cm^3 Amp.

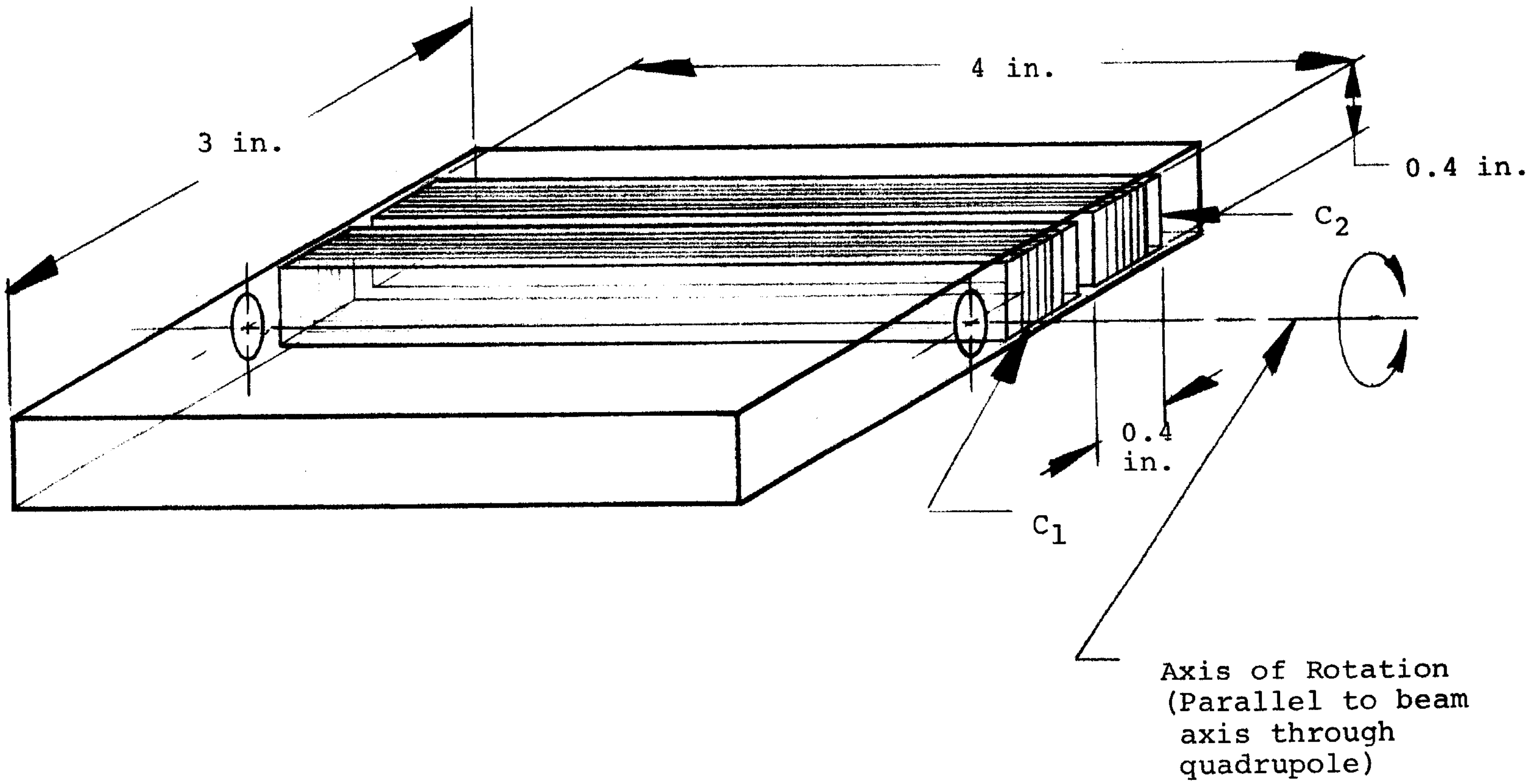

Figure 1   Search coil assembly

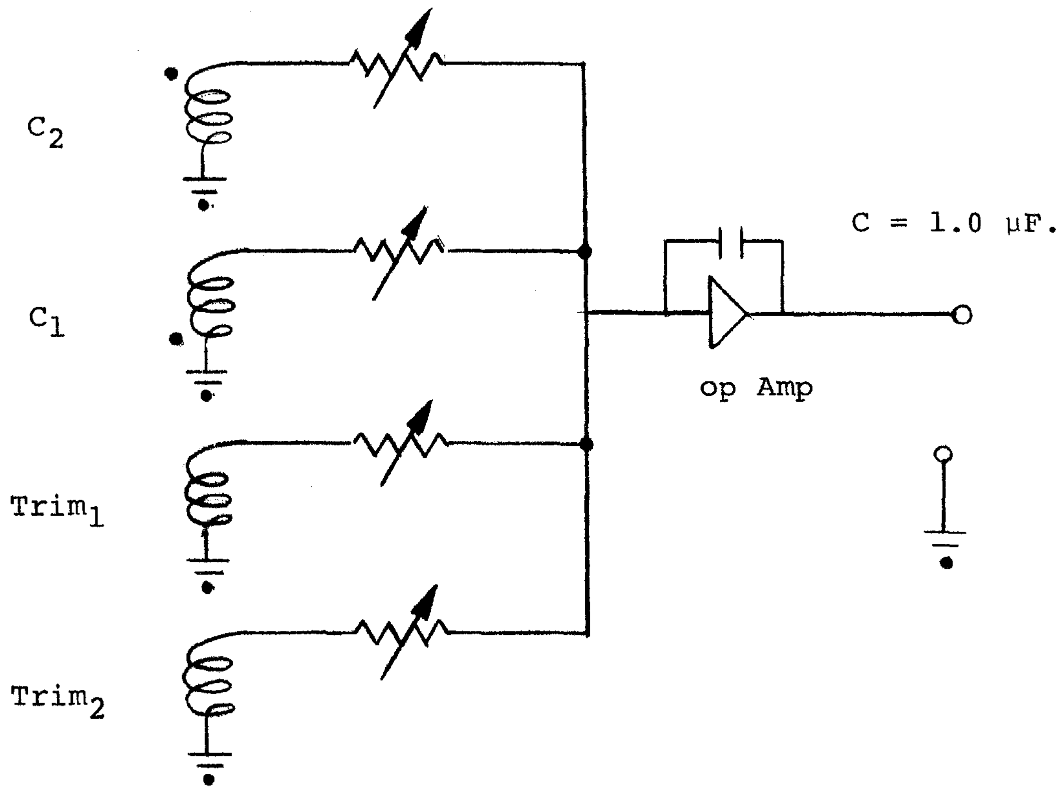

Resistance of each <u>arm</u>

R_2 = 1126 Ω
R_1 = 500 Ω
R_{T1} = 641 Ω
R_{T2} = 613 Ω

Figure 2 Search coil and integrator schematic

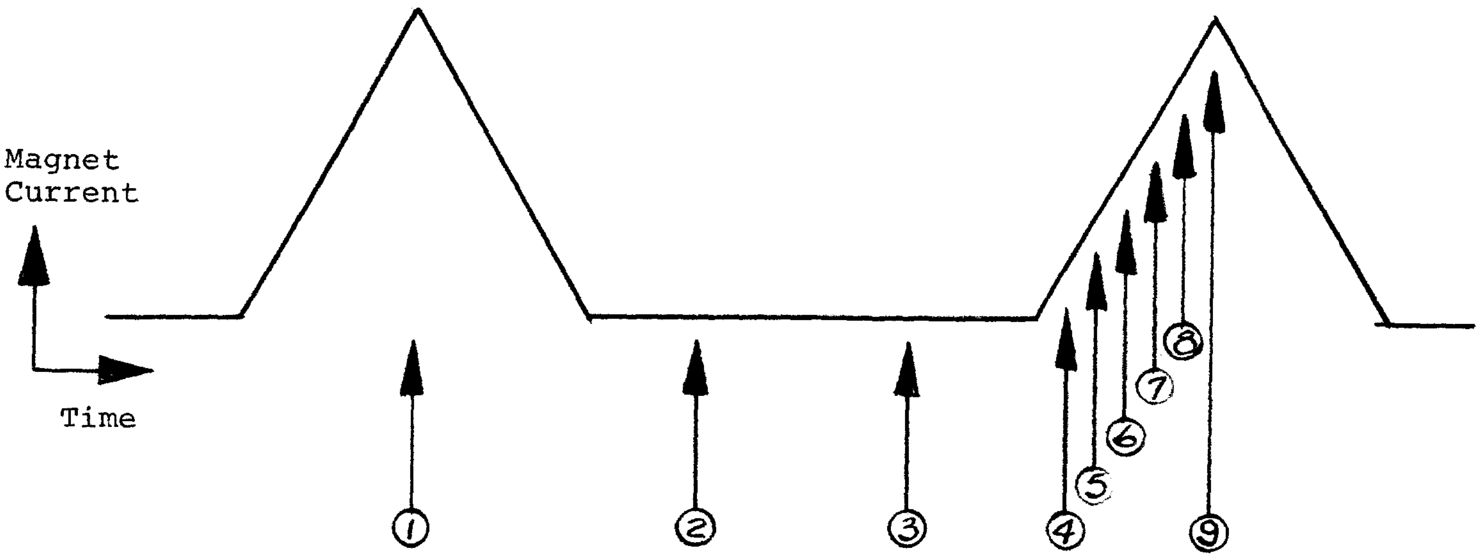

1. Peak of excitation. Stepping motor pulsed; 2 second wait initiated.
2. Drift measurement started.
3. One second later. Drift measurement finished.
4. First preselected excitation level reached. Output voltage of measuring circuit (Fig. 2) read.
5. thru 8. Second thru fifth excitation levels. Same action as at 4.
9. Peak of excitation. Same action as 1.

The period of the cycle (1. to 9.) was 10 sec.

Figure 3 Measuring Cycle
followed by the computer

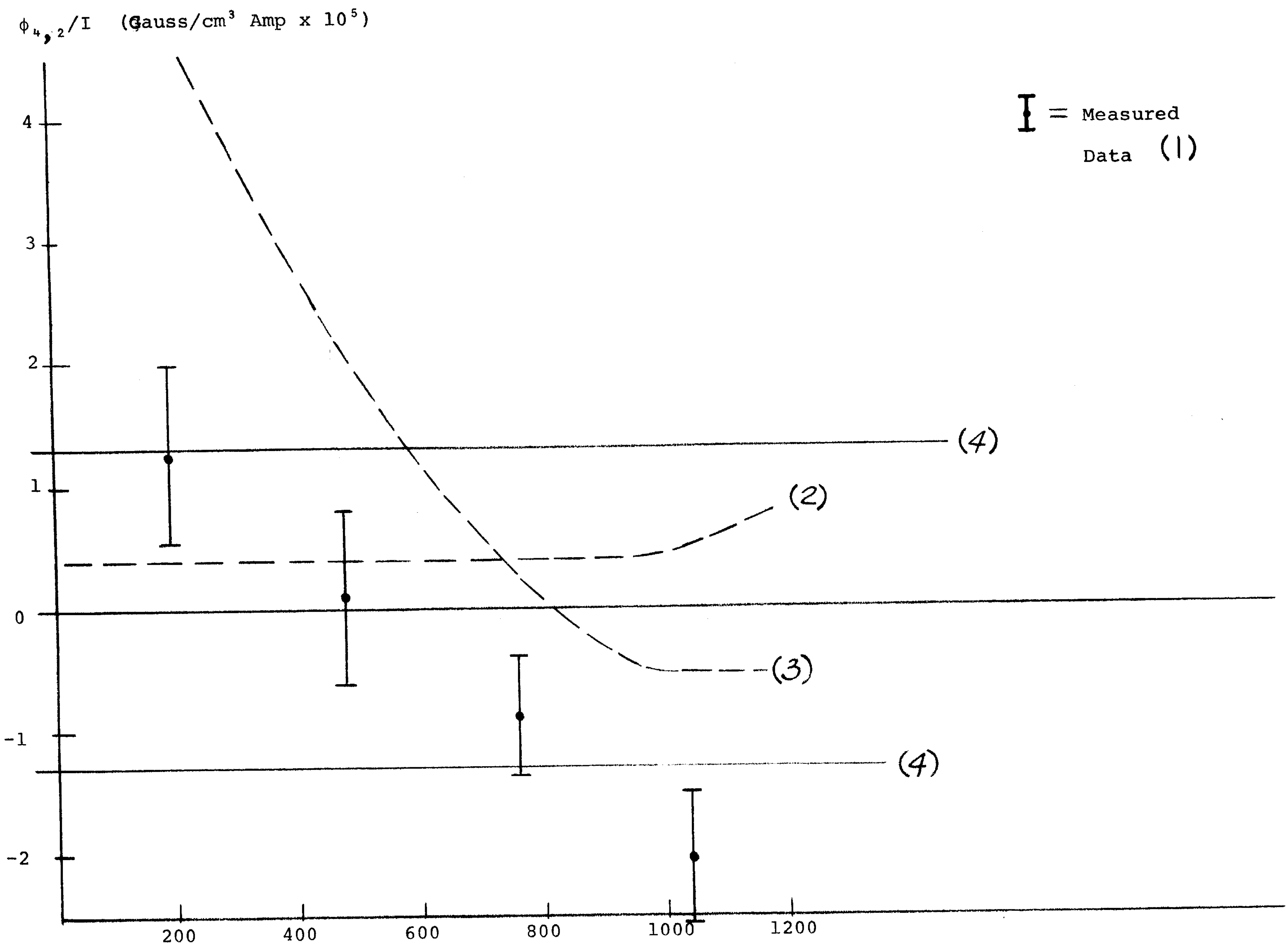

Figure 4 Octupole Coefficients (For explanation of numbers, see text)